

# Supplemental Material: A Hyperspectral Space of Skin Tones for Inverse Rendering of Biophysical Skin Properties

Carlos Aliaga<sup>1</sup>  Menqi Xia<sup>1,2</sup>  Xiao Xie<sup>1</sup>  Adrian Jarabo<sup>1</sup>  Gustav Braun<sup>1</sup>  Christophe Hery<sup>1</sup> 

<sup>1</sup>Meta Reality Labs Research    <sup>2</sup>EPFL

## Abstract

This is the supplemental material for the paper A Hyperspectral Space of Skin Tones for Inverse Rendering of Biophysical Skin Properties. It includes further analysis of the albedo space (Section 1); a discussion and tests of Kubelka-Munk to compute diffuse reflectance (Section 2), a discussion of the Look Up Tensor approach (Section 3); other implementation and rendering details (Section 4); more comparisons with related work (Section 5); and further results (Section 6).

## CCS Concepts

• Computing methodologies → Reflectance modeling; Reconstruction;

## 1. Albedo Space Analysis. Further details

In spectral color modeling, it is efficient to represent a large spectral dataset using principal component analysis (PCA) with a lower number of dimensions [TB05]. Based on the first three principal components trained from our spectral dataset, in Figure 1, the PCA reconstructed spectra of some representative Leeds spectra are compared with the original measurements. The bottom shows the histogram of the reconstruction root mean squared errors. In addition to the Leeds dataset that only has the visible wavelength range, the IR range up to 1000 nm is tested using the NIST dataset [CA13], which has less data points and skin varieties though. Both datasets can be accurately represented (less than 0.03 RMSE) via the three principle components from our spectral manifold.

## 2. Kubelka-Munk

For computing the diffuse reflectance of a skin patch, we first started by using a Kubelka-Munk (KM) [KM31] layering model, following previous work [AS17].

We experimented through different variations of the KM-based model, all of them suffering from lack of expressiveness and requiring many ad-hoc parameters to tune the layering quantities. These issues with KM approaches stem mostly from the fact that the theory was initially derived for pigments, and it is known to exhibit some limitations, like inaccuracies in cases of dark shades or thin films [Cho14], that can make this technique not adequate in our context.

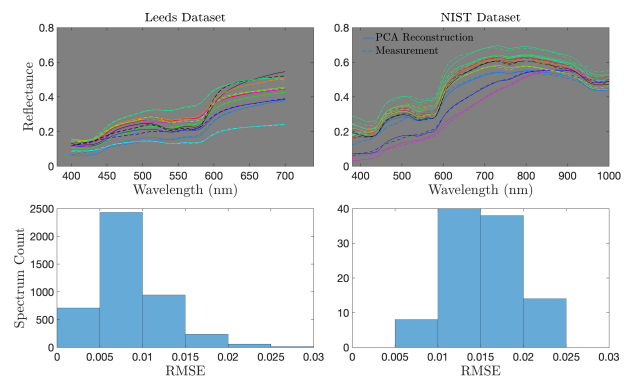


**Figure 1:** PCA reconstructions for the Leeds and NIST datasets. Top rows show some representative spectral comparisons between the reconstructions using the PCA basis functions from our spectral manifold versus the spectrophotometric measurements. Bottom row show the histograms of the reconstruction RMSE across the two dataset.

Moreover, there is no clear conversion between the parameters of Radiative Transfer and those of KM theories. We tested existing empirical relationships [RRG12] and more grounded derived ones from optics literature [SK14]. Unfortunately, the model is still unable to generalize to various skin types, lacks fidelity in certain areas such as the lips, and other heterogeneities (imperfections) are not really recovered (see Figure 2).

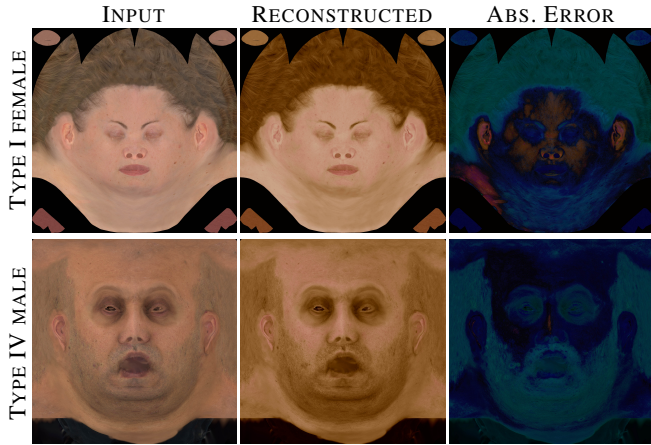


**Figure 2:** Reconstruction results using a Kubelka-Munk based model [AS17] for different types of skin. The model is unable to recover the original albedo from the inferred properties (only melanin and haemoglobin volume fractions in this case), leading to noticeable shifts in the skin shades.

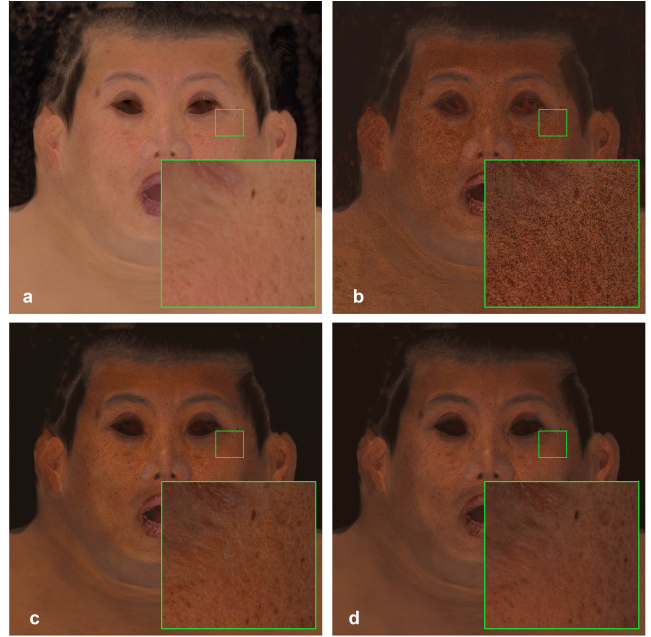


**Figure 3:** The LUT approach suffers from quantization in the estimated parameters maps even for large tensors. This issue does not reveal during reconstruction, but creates artifacts and even some perceptual color shifting when edits on the skin properties are performed. An example of a  $\times 3$  edit over the reconstructed melanin concentration of a Type III skin is shown. From left to right: a) original image, and reconstructions (edited melanin  $\times 3$ ) using a b) tensor of 55296 skin tones  $(V_m, V_b, t, \Phi_m, \Phi_h) = (64, 32, 3, 3, 3)$ , c) tensor of 256k skin tones  $(64, 32, 5, 5, 5)$ , d) learned inverse mapping using 600k points to train the network. Whereas even for densely sampled tensors quantization appears, the neural approach provides smooth maps for the estimated parameters, which results in clean edits.

### 3. Recovering the Skin Properties using a Look-up Tensor

We pre-compute a wide tensor of skin tones by following the sampling strategy outlined in the paper. To estimate the skin parameters given an input albedo, we search the LUT on each texel of the albedo to find the best skin parameter set that minimizes a reconstruction  $L_2$  error. Then, we can manipulate them and query the new corresponding albedo from the LUT. This approach is able to reconstruct the skin albedo faithfully with an error close to zero. However, the inverted parameter maps are noisy and have many discontinuities, since the mapping from RGB to skin parameters is not smooth. In turn, editing operations over neighboring pixels in such extracted components can lead to unexpected abrupt changes in the reconstructed albedos (see Figure 3). We leave out of scope of this paper the assessment of different representations or data structures suitable for more efficient search strategies, that could dramatically improve the performance of this approach.

### 4. Implementation Details and Decisions on the Model

**Using the model In Rendering** In the spirit of a well known technique in production [WVH17], to preserve the skin details coming from the albedo texture, we make use of the reconstructed and edited albedo maps and compute a 3D random walk subsurface scattering solution that relies on a numerical albedo inversion around the mean free path and accounting for the anisotropy factor  $g$  (see Figure 4).

**Using Albedo Maps in Rendering.** The final 3D lit geometries of our virtual faces are rendered using our own skin materials inside *Blender Cycles* [Ble20]. Aside from the specular component of the skin, which we represent as a double lobe GGX [WMLT07], we follow, in the spirit of a state of the art technique in production [WVH17], a 3D random walk subsurface scattering solution that relies on a numerical albedo inversion around the mean free

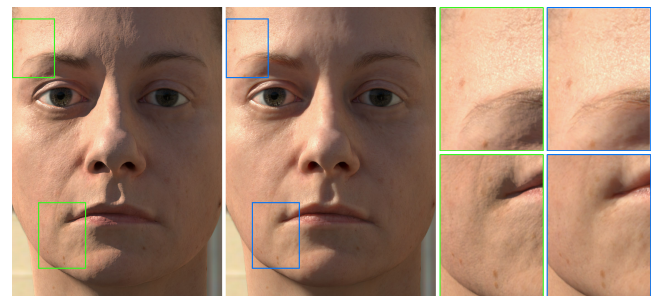


**Figure 4:** Lambertian vs Random Walk Subsurface Scattering in final rendering stage. The numerical albedo inversion allows to drive the attenuation by the albedo map, ensuring skin details are preserved and not over blurred by the 3D SSS simulation.

path and accounting for the anisotropy factor  $g$ . At this stage, we simplify the model to be single layered, dermis and epidermis combined, as a semi infinite medium. Obviously multi-layered models could be employed, for instance directly consuming the chromophores estimations, but these are out of scope of this paper. See

69 Figures 7, 8, and 9 for examples of path traced renders under 3  
70 different lighting environments.

## 71 5. Further Comparisons with Previous Work

72 We conduct a series of comparisons with the related and recent  
73 work from [GGD\*20]. Not having access to the trained models, we  
74 run our method over the the paper's images, skin patches obtained  
75 via the Antera device (under D65 illuminant) in Figure 5.

## 76 6. Further Results

77 We perform estimations and manipulations of skin parameters over  
78 several skin types covering the Fitzpatrick scale [Fit88]. With the  
79 LUT approach, using the largest tensor (256k skintones) resulted in  
80 varying times from 2 to 5 hours for 2k by 2k images, or more than  
81 7 hours for 4k by 4k images, using brute force multi threaded (12)  
82 search on the tensor in an Intel Xeon W-2135 at 3.70GHz. We refer  
83 the readers to Figure 3, that showcases the problems of LUTs.

84 *Robustness under different illuminants* For completeness, we in-  
85 clude in Figure 6 the complete set of estimated properties for the  
86 two faces under 4 color temperatures shown in Figure 9 of the pa-  
87 per.

88 *Editing the Skin Parameters* We show how we can manipulate di-  
89 rectly in this space of inferred skin properties, scaling some of them  
90 up or down in an intuitive and predictable manner. We run the neu-  
91 ral decoder on these modified quantities to reconstruct biophysical  
92 albedos, and finally render them on 3D faces. For skin types rang-  
93 ing from I to V, we perform large edits in hemoglobin and melanin  
94 content, with details explained in Figure 7, 8 and 9. Note the ed-  
95 its are naive in order to cover similar ranges for all skin types, and  
96 the RGB version of the model was used for these manipulations, so  
97 extreme edits can turn unnatural.

## 98 References

- 99 [AS17] ALOTAIBI, SARAH and SMITH, WILLIAM AP. "A biophysical 3D  
100 morphable model of face appearance". *Proceedings of the IEEE Interna-*  
101 *tional Conference on Computer Vision Workshops*. 2017, 824–832 1, 2.
- 102 [Ble20] BLENDER ONLINE COMMUNITY. "Blender: a 3D modelling and  
103 rendering package". (2020). URL: <http://www.blender.org> 2.
- 104 [CA13] COOKSEY, CATHERINE C and ALLEN, DAVID W. "Reflectance  
105 measurements of human skin from the ultraviolet to the shortwave  
106 infrared (250 nm to 2500 nm)". *Active and Passive Signatures IV*.  
107 Vol. 8734. SPIE. 2013, 152–160 1.
- 108 [Cho14] CHOUDHURY, ASIM KUMAR ROY. *Principles of colour and ap-*  
109 *pearance measurement: Object appearance, colour perception and in-*  
110 *strumental measurement*. Elsevier, 2014 1.
- 111 [Fit88] FITZPATRICK, THOMAS B. "The validity and practicality of sun-  
112 reactive skin types I through VI". *Archives of dermatology* 124.6  
113 (1988), 869–871 3.
- 114 [GGD\*20] GITLINA, YULIYA, GUARNERA, GIUSEPPE CLAUDIO,  
115 DHILLON, DALJIT SINGH, et al. "Practical Measurement and Recon-  
116 struction of Spectral Skin Reflectance". *Computer Graphics Forum*.  
117 Vol. 39. 4. Wiley Online Library. 2020, 75–89 3, 4.

- 118 [KM31] KUBELKA, PAUL and MUNK, FRANZ. "An article on optics of  
119 paint layers". *Z. Tech. Phys* 12.593-601 (1931), 259–274 1.
- 120 [RRG12] ROY, ARINDAM, RAMASUBRAMANIAM, RAJAGOPAL, and  
121 GAONKAR, HARSHAVARDHAN A. "Empirical relationship between  
122 Kubelka-Munk and radiative transfer coefficients for extracting optical  
123 parameters of tissues in diffusive and nondiffusive regimes". *Journal of*  
124 *biomedical optics* 17.11 (2012), 115006 1.
- 125 [SK14] SANDOVAL, CHRISTOPHER and KIM, ARNOLD D. "Deriv-  
126 ing Kubelka–Munk theory from radiative transport". *JOSA A* 31.3  
127 (2014), 628–636 1.
- 128 [TB05] TZENG, DI-YUAN and BERNS, ROY S. "A review of principal  
129 component analysis and its applications to color technology". *Color Re-*  
130 *search & Application* 30.2 (2005), 84–98 1.
- 131 [WMLT07] WALTER, BRUCE, MARSCHNER, STEPHEN R., LI, HONG-  
132 SONG, and TORRANCE, KENNETH E. "Microfacet Models for Refrac-  
133 tion through Rough Surfaces". *Proceedings of the 18th Eurographics*  
134 *Conference on Rendering Techniques*. EGSR'07. Grenoble, France: Eu-  
135 rographics Association, 2007, 195–206. ISBN: 9783905673524 2.
- 136 [WVH17] WRENNINGE, MAGNUS, VILLEMIN, RYUSUKE, and HERY,  
137 CHRISTOPHE. *Path traced subsurface scattering using anisotropic phase*  
138 *functions and non-exponential free flights*. Tech. rep. Technical Memo,  
139 2017 2.

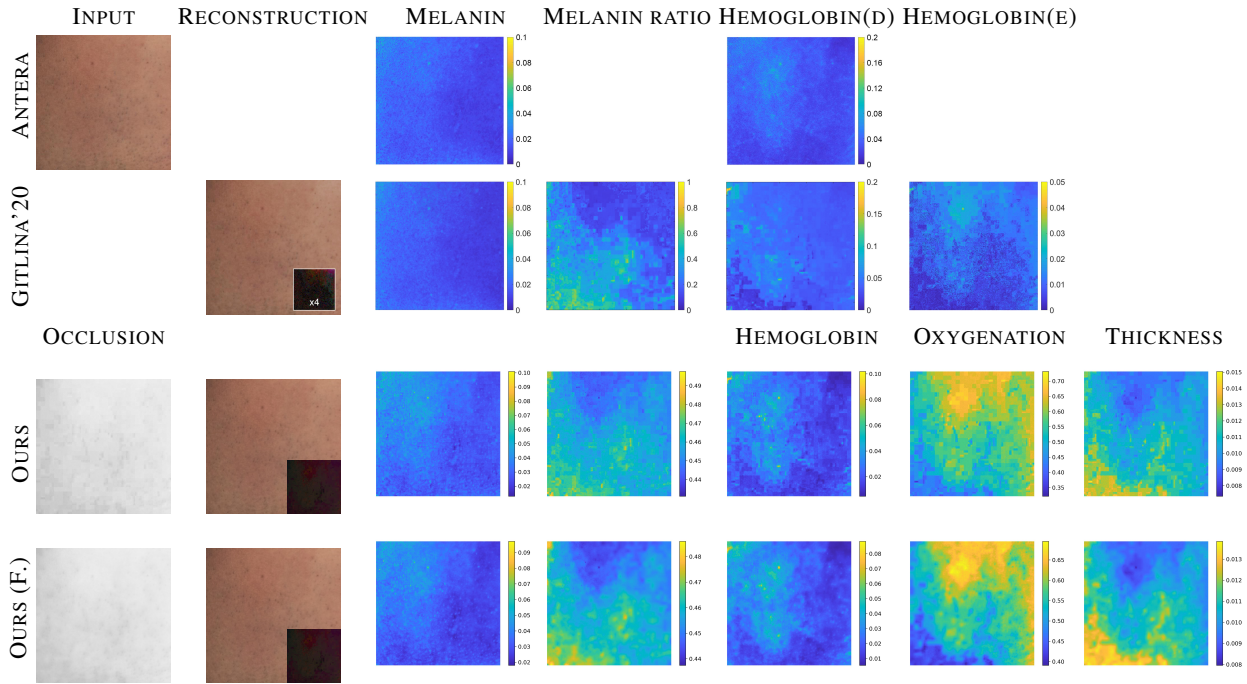


**Figure 5:** Comparison with the skin albedo patch from [GGD\*20]. Top: their reconstruction ( $MSE = 0.0130$ ) and estimated parameters. Middle: ours ( $MSE = 1.26 \times 10^{-05}$ ). Note that the image contains compression and color artifacts, and does not seem to have an homogeneous lighting. This causes an excess of estimated melanin concentration (higher even in our reconstruction), in reference to what seems appropriate for that type of skin. Interestingly, the level of oxygenation appears to correlate with the extended blood concentration in the epidermis from their work. Bottom: our reconstruction over a filtered input (after removal of spatial and color JPEG artifacts).

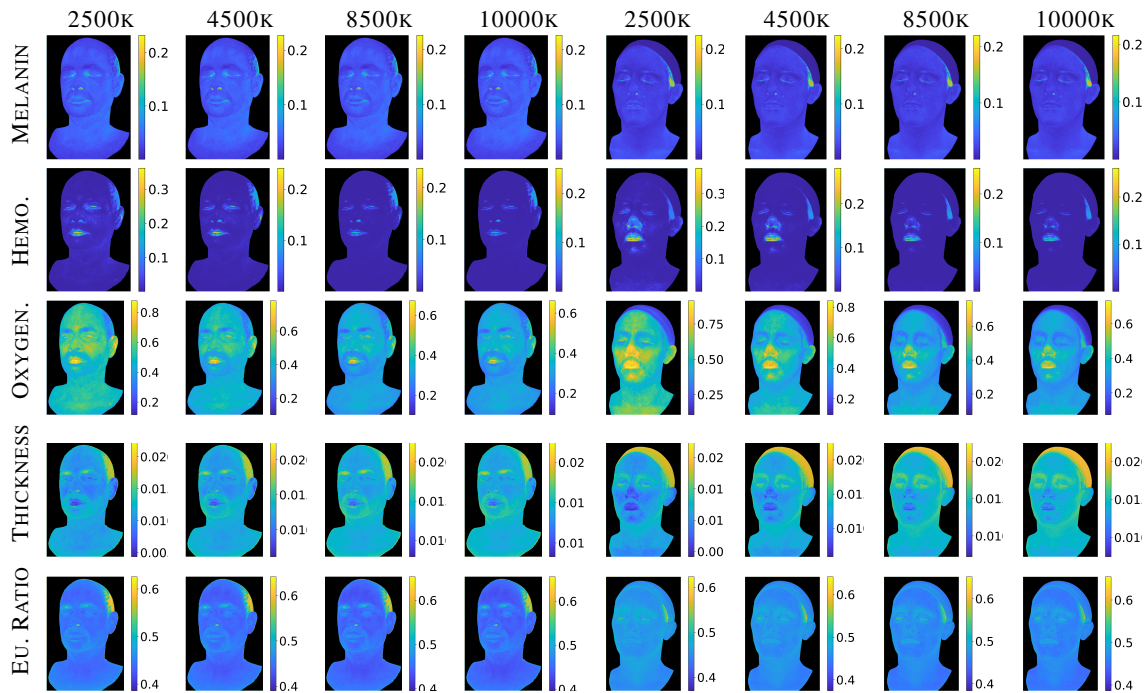


**Figure 6:** Complete estimated skin properties for the faces under different color temperatures shown in the paper.



**Figure 7:** Rendering results under our most neutral lighting scenario for edited skin parameters inferred by our model over different skin types (classified according to the Fitzpatrick scale). From left to right, original, followed by different manipulations per subject, three in blood concentration and three in melanin concentration. Note that these are straight algebraic edits on the recovered skin components, with no additional artistic tweaks or touch-ups involved. Though they demonstrate that our skin model describes an expressive reflectance space, these naive edits can result sometimes in semi non natural skins.

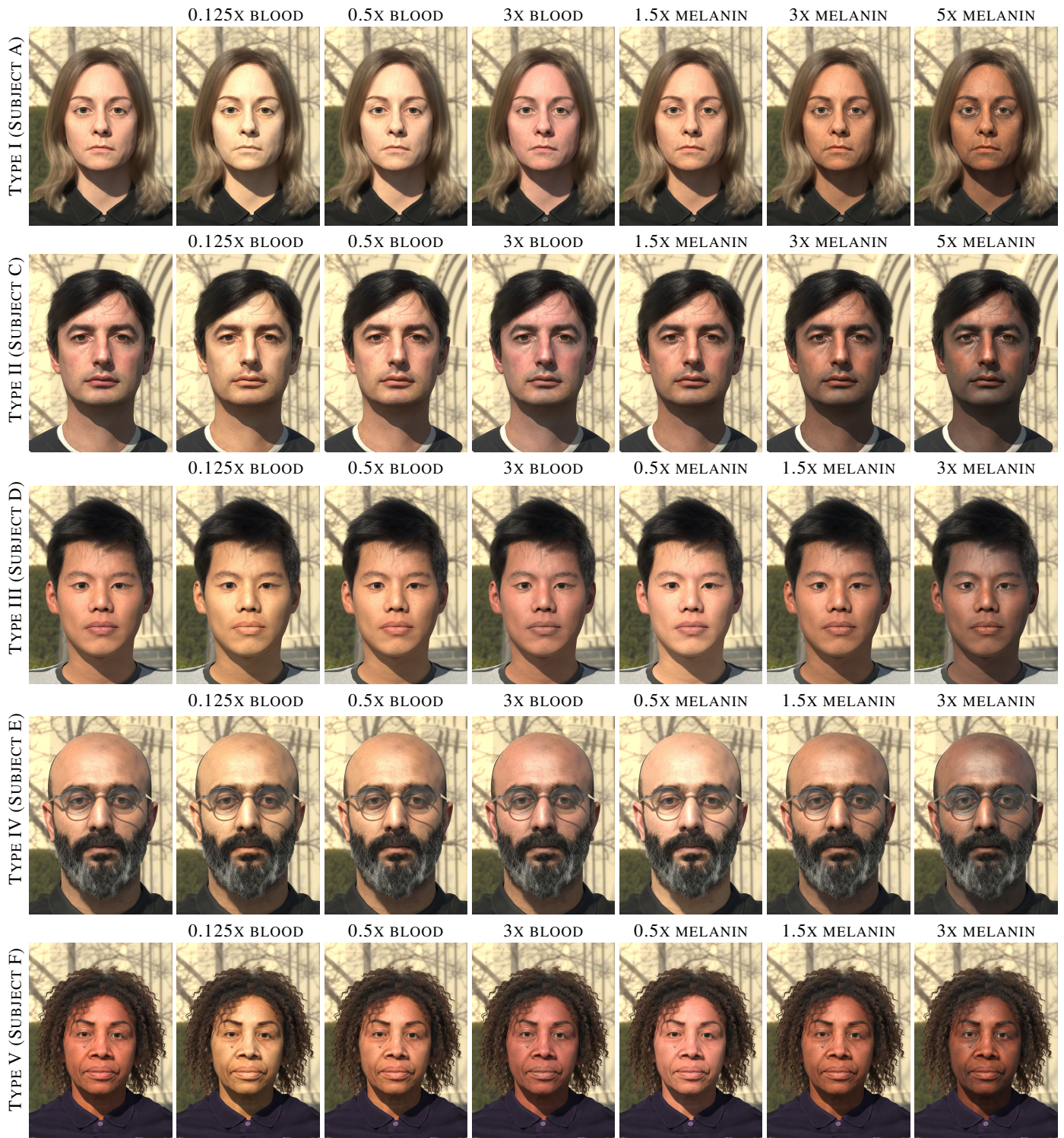


**Figure 8:** Rendering results under lighting scenario 2 for edited skin parameters inferred by our model over different skin types. From left to right, original, followed by different manipulations per subject, three in blood concentration and three in melanin concentration.

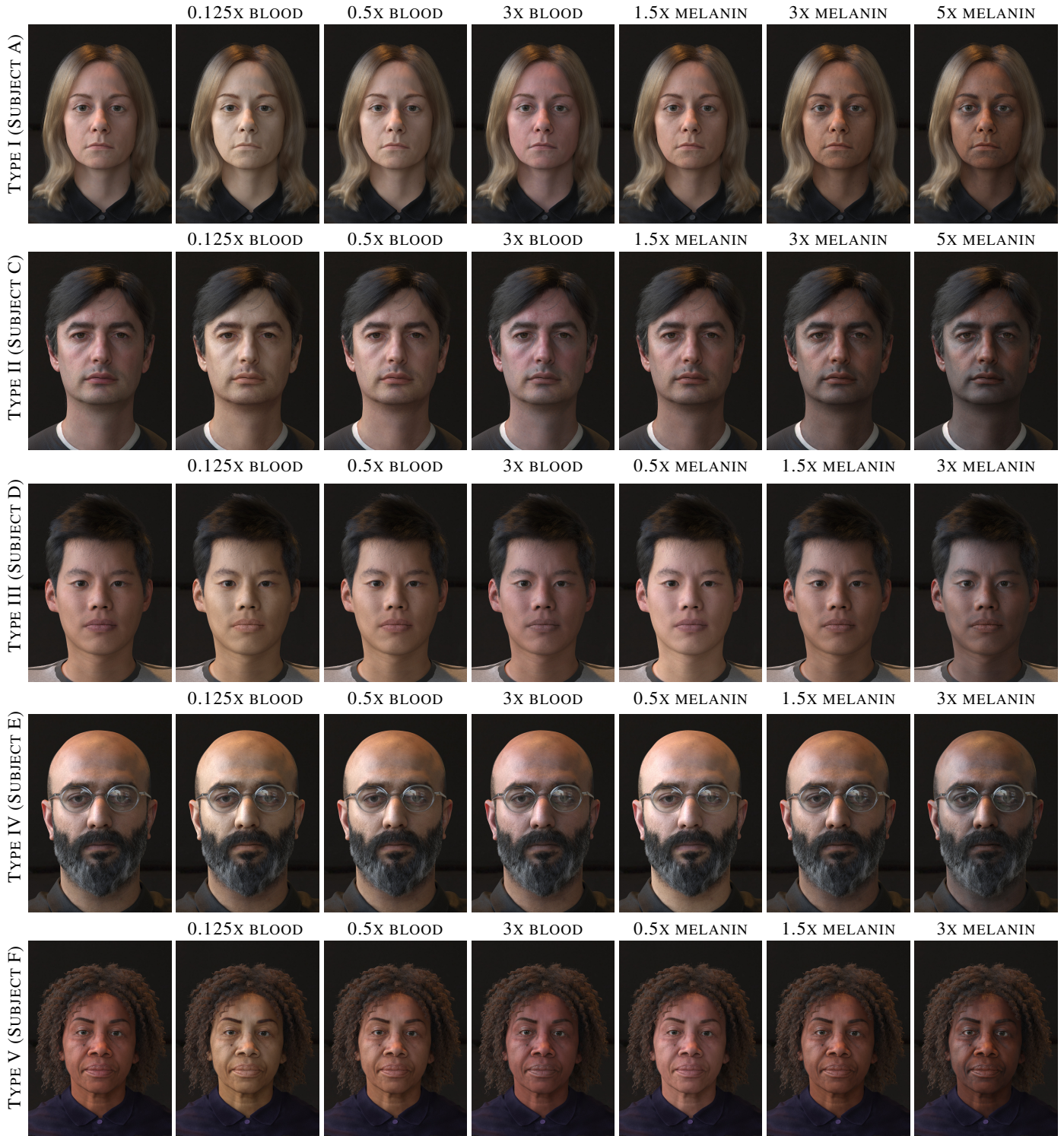


**Figure 9:** Rendering results under lighting scenario 3 for edited skin parameters inferred by our model over different skin types. From left to right, original, followed by different manipulations per subject, three in blood concentration and three in melanin concentration.